Interaction of HIV protease inhibitors with OATP1B1, 1B3 and 2B1

Pieter Annaert [1], Zhi-wei Ye [1], Bruno Stieger [2], and Patrick Augustijns[1]*

1. Laboratory for Pharmacotechnology and Biopharmacy, Department of Pharmaceutical Sciences, Katholieke Universiteit Leuven, O&N2, Herestraat 49-bus-921, 3000 Leuven (Belgium).

2. Division of Clinical Pharmacology and Toxicology, Department of Medicine, University Hospital, 8091 Zürich (Switzerland)

* Corresponding author:

Pieter P. Annaert

Laboratory for Biopharmacy and Pharmacotechnology, Department of Pharmaceutical Sciences, Katholieke Universiteit Leuven

O&N2, Herestraat 49 – bus 921, 3000 Leuven (Belgium)

Tel: +32-16–330303 Fax: +32-16–330305

e-mail: Pieter. Annaert@pharm.kuleuven.be

Key words: hepatic drug transport, OATP, HIV protease inhibitor, drug interaction

Abbreviations: Chinese Hamster Ovary (CHO), Organic Anion Transporting Polypeptide [Oatp(rat), OATP(human)], Fetal Bovine Serum (FBS), Hanks' Balanced Salt Solution (HBSS), Phosphate Buffered Saline (PBS), Cholyl-Glycylamido-Fluorescein (CGamF), Protease Inhibitors (PI)

Abstract

1. The effects of HIV protease inhibitors (PI) on accumulation of the fluorescent bile salt analogue cholyl-glycylamido-fluorescein (CGamF) were determined in OATP1B1- and 1B3-expressing CHO cells. In addition, interaction studies in Caco-2 monolayers, known to only express the OATP2B1 isoform, were conducted using the established OATP substrate estrone-3-sulfate (E3S), since no CGamF accumulation was observed in Caco-2 monolayers. 2. CGamF appeared an excellent substrate for the OATP1B subfamily, with net accumulation clearance values of 7.8 and 142 µl/min/mg protein in 1B1 and 1B3-transfected cells, respectively. K_i values reflecting inhibition of CGamF accumulation by HIV PI correlated well between OATP1B1 and 1B3-expressing cells. Lopinavir was the most potent inhibitor (K_i 0.5-1.4 µM) of OATP1B-mediated CGamF accumulation, compared to atazanavir, darunavir, ritonavir and saquinavir (K_i between 1.4 and 3.3 µM). 3. Inhibitory profiles towards OATP2B1-mediated E3S accumulation were different with only indinavir, saquinavir and ritonavir showing substantial effects. 4. In conclusion, OATP1B3 appears to be a major transport mechanism mediating sodium-independent CGamF accumulation in human liver and CGamF could be used as a probe substrate for *in vitro* drug interaction studies. The remarkably potent inhibition of OATP1B1 by lopinavir may explain some clinically relevant drug interactions between lopinavir and OATP1B substrates such as fexofenadine.

Organic anion transporting polypeptides (OATP/Oatp, Human/Rat, *SLCO/Slco*) belong to a growing superfamily of transporters that mediate cellular accumulation of structurally diverse amphiphilic organic solutes (Hagenbuch and Gui, 2008). Eleven human OATP isoforms and 14 rat Oatp isoforms have thus far been identified. OATP1B1, OATP1B3 and OATP2B1 are the three human OATPs that are now considered to play a crucial role in hepatic uptake of exogenous and endogenous compounds at the liver sinusoidal membrane domain. OATP1B1 and 1B3 are liver-specific, whereas OATP2B1 displays wide tissue distribution (Annaert et al., 2007).

Many drugs have been identified as OATP substrates and clinical drug interactions that can be attributed to the OATP inhibition have been observed (Konig et al., 2006; Hagenbuch and Gui, 2008). For example, heart transplant patients receiving cyclosporine and rosuvastatin showed a sevenfold increase in rosuvastatin AUC as compared to historical controls (Simonson et al., 2004). On the other hand, rosuvastatin exhibits no drug interaction when coadministered with the potent CYP3A4 inhibitor ketoconazole (Cooper et al., 2003). Rosuvastatin is not transported by the canalicular transporters MDR1 (ABCB1) or MRP2 (ABCC2) (Huang et al., 2006), however interference with its OATP-mediated hepatic uptake was found to contribute significantly to the marked interaction with cyclosporin. Apart from OATP-mediated drug interactions, interindividual variability in genes encoding OATP transporters can also result in marked interindividual differences in pharmacokinetics; the impact of OATP1B1 polymorphisms has been extensively documented. For example, a single-nucleotide polymorphism (c.521T>C, P.Val174Ala) in the *SLCO1B1* gene encoding OATP1B1 decreases the ability of OATP1B1 to transport simvastatin, resulting in markedly increased plasma concentrations of simvastatin and an enhanced risk of simvastatin-induced myopathy (Link et al., 2008). The *SLCO1B1* polymorphism also has implications regarding the hepatic uptake of bile acids *in vivo* in human (Xiang et al., 2009).

These examples illustrate that mechanisms underlying hepatic drug interactions frequently extend beyond the classical involvement of P450-mediated drug metabolism (DuBuske, 2005; Endres et al., 2006). In addition, since endogenous compounds such as bile salts rely on hepatic transporters to maintain normal hepatic physiology (e.g., bile flow), drugs that inhibit the function of key transporters may also cause important disturbances of endogenous substance elimination via the hepatobiliary system.

The use of probe substrates and inhibitors to determine the relative importance of individual hepatic transporters has advanced the value of uptake data obtained using hepatocytes in drug discovery (Soars et al., 2007). However, as discussed by Wang et al. (Wang et al., 2008), although the use of selective inhibitors of efflux transporters can provide useful mechanistic information on drug interactions involving efflux transporters, the potential cross-reaction of inhibitors with multiple transporters makes it difficult to discern the role of individual transporters in drug transport. For instance, MK 571 has been considered a specific inhibitor for MRP2 (Gekeler et al., 1995), but some studies have indicated that it can also inhibit uptake transporters OATP1B1, 1B3 and 2B1 (Yamazaki et al., 2005; Letschert et al., 2006). Elacridar was originally synthesized to be a selective inhibitor for MDR1 (Wallstab et al., 1999), but was found to also potently inhibit BCRP (ABCG2) (de Bruin et al., 1999).

It follows that continuing efforts are required to identify and thoroughly profile new transporter probe substrates and inhibitors. In this context, we recently reported on the characterization of the hepatic disposition of the bile salt analog cholyl-glycylamido-fluorescein (CGamF) in animal and human hepatocytes (Ye et al., 2008; Ye et al., 2009). CGamF was synthesized by conjugation of 5-aminofluorescein with the carboxylic group of the natural bile acid cholylglycine yielding a fluorescent bile salt analogue (Holzinger et al., 1998). The utility of CGamF as a convenient

fluorescent probe simulating bile salt transport in various *in vitro* and *in vivo* models of different species has been demonstrated previously (Maglova et al., 1995; Bravo et al., 1998; Holzinger et al., 1998; Mita et al., 2006). Mita et al. (2006) showed that CGamF as well as other fluorescent bile salt analogues were transported across LLC-PK1 cells co-expressing NTCP (SLC10A1) and BSEP (ABCB11), albeit at a substantially lower rate than the natural bile salt taurocholate. In rat and human hepatocytes, we demonstrated that CGamF is mainly accumulated by sodium-independent mechanisms that are sensitive to the OATP inhibitor rifampicin (Ye et al., 2008; Ye et al., 2009). Coincubation of CGamF with digoxin (to inhibit OATP1B3 in human and Oatp1a4 in rat (Annaert et al., 2007)), caused some inhibition but less than following coincubation with rifampicin in rat and human, indicating that at least OATP1B3/Oatp1a4 is involved in the hepatic uptake of CGamF in the human/rat liver. However, while these data strongly support a pivotal role of OATPs in CGamF accumulation, the relative contribution of the three OATP isoforms that are expressed in the basolateral membrane of hepatocytes (OATP1B1, OATP1B3 and OATP2B1) are not known.

A range of expression systems have been utilized to investigate the substrate specificity of OATPs, including *Xenopus laevis* oocytes injected with complementary RNA (Hagenbuch et al., 1996) and stable transfections of OATPs in cell lines such as Chinese Hamster Ovary (CHO) cells (Treiber et al., 2007; Gui et al., 2008). In addition, the well known Caco-2 cell line shows substantial expression of OATP2Bl in the apical membrane, where it contributes predominantly to the accumulation of E3S, thus making Caco-2 cells an attractive *in vitro* tool for assessing OATP2B1-mediated drug-drug interactions (Sai et al., 2006).

In the present study, we expanded our previous *in vitro* data obtained in animal and human hepatocytes by conducting CGamF transport and interaction experiments in OATP1B1 and 1B3 transfected CHO cells. In addition, E3S was used as model substrate for the OATP2B1-mediated

interaction with HIV PI since CGamF did not accumulate in Caco-2 cells.

Materials and Methods

Chemicals. Amprenavir was kindly provided by GlaxoSmithKline (Middlesex, UK). Ritonavir, indinavir sulfate, saquinavir mesylate, nelfinavir mesylate and lopinavir were donated by Hetero Drugs Limited (Hyderabad, India). Atazanavir was obtained from Bristol-Myers Squibb (New Brunswick, NJ) and darunavir was obtained from Cilag AG (Switzerland). HEPES (4-(2-hydroxyethyl)-1-piperazineethanesulfonic acid) was purchased from MP Biomedicals (Illkirch, France). Dulbecco's Modified Eagle Medium (DMEM) (containing 1 g/l D-glucose, 1 mM L-glutamine, 25 mM HEPES buffer and 110 mg/l sodium pyruvate) and Geneticin G-418 were from Invitrogen (Paisley, UK), L-Glutamine, Penicillin-streptomycin-mixture (contains 10,000 units potassium penicillin and 10,000 µg streptomycin sulfate per ml in 0.85 % saline), Fetal Bovine Serum (FBS), Hanks' Balanced Salt Solution (HBSS) and Phosphate Buffered Saline 1× (PBS) were purchased from Lonza Verviers SPRL (Verviers, Belgium). L-proline, sodium butyrate, estrone-3-sulfate, digoxin, rifampicin, rifamycin SV, bromsulphophthalein and Triton X-100 were purchased from Sigma-Aldrich (Schnelldorf, Germany). Cholyl-glycylamido-fluorescein was kindly provided by Prof. Alan Hofmann (University of California, San Diego). ^{3}H-estrone-3-sulfate (E3S; 57.3 Ci/mmol) was obtained from PerkinElmer Life Sciences (Boston, MA). All other chemicals and reagents were of analytical grade and were readily available from commercial sources. CHO cells expressing OATP1B1 and OATP1B3 have been described previously (Treiber et al., 2007; Gui et al., 2008).

Cell culture. OATP1B1 and OATP1B3-transfected CHO cells and the wild-type cells were cultured at passage 40 to 60. Wild-type cells were grown at 37°C in 75 cm^2 T-flasks in a humidified 5% CO_2 atmosphere in DMEM containing 1 g/l D-glucose, 1 mM L-glutamine, 25 mM HEPES and 110 mg/l sodium pyruvate, supplemented with 10% FBS, 50 µg/ml L-proline, 100 IU/ml penicillin,

100 µg/ml streptomycin. The culture medium for the transfected cell lines additionally contained geneticin (G-418, 500µg/ml). For accumulation experiments CHO-wild-type and OATP-expressing cells were plated at 40,000 cells per well on 24-well plates and culture medium was replaced every other day. Accumulation experiments were performed on day 4 to 5 after seeding when cells were grown to confluence. One day before starting the accumulation experiments, cells were additionally treated with 5 mM sodium butyrate. Caco-2 cells were purchased from Cambrex Biosciences (Walkersville, MD) and grown in 75 cm^2 culture flasks at 37 °C in an atmosphere of 5% CO_2 and 90% relative humidity. Cells were passaged every 3-4 days (at 70-80% confluence) at a split ratio of 1-7. For transport experiments, Caco-2 cells were plated at a density of 40,000 per well on 24-well plates. Confluence was reached within 3-4 days after seeding and the monolayers were used for the experiments 2 weeks post-seeding. Cell passages between 50 and 70 were used in the experiments.

Accumulation studies. Cells were rinsed twice with 0.5 ml/well of standard buffer (Hanks' Balanced Salt Solution with 10 mM HEPES, pH 7.4) and pre-incubated for 10 min at 37°C. For experiments in which the effect of inhibitors was investigated, cells were pre-incubated for 10 min with 0.5 ml of the standard buffer containing the inhibitor at desired concentration. Subsequently, 0.5 ml of double-concentrated substrate solution was added to initiate the actual incubation. After the incubation, cells were rinsed four times with 1 ml of ice-cold standard buffer and lysed with 0.5 ml of 0.5% Triton X-100 solution (in PBS) by placing plates on a shaker for 20 min at room temperature. Cell lysates were analyzed by fluorescence spectroscopy (ex 490 nm; em 524 nm) in a Tecan Infinite M200 plate reader (Austria) for determination of CGamF concentrations, and by liquid scintillation spectroscopy (Wallac 1410, Finland) for ^{3}H-E3S. Accumulation was normalized to the protein content of the CHO cells and Caco-2 cells in each well which was measured by using

the BCA™ Protein Assay kit (Pierce Chemical, Rockford, IL). All accumulation data were corrected for nonspecific binding to cell-free culture plates. Accumulation values in transfected CHO cells were corrected by subtracting accumulation into non-transfected CHO cells.

Data analysis.

For the characterization of E3S accumulation kinetics in Caco-2 cells, the following equation was used:

$$V = K_d.C + \frac{V_{max1}.C}{K_{m1} + C} + \frac{V_{max2}.C}{K_{m2} + C}$$

with K_d representing the rate constant for the nonsaturable accumulation, and K_m and V_{max} representing the kinetic parameters for the saturable (Michaelis-Menten) accumulation components. This equation was used based on previous data reflecting E3S accumulation in Caco-2 cells (Sai et al., 2006). The Michaelis-Menten equation was fitted to the data of net accumulation of CGamF in transfected CHO cells. All the parameters were obtained by using the Solver tool in Microsoft Excel 2003.

In addition, the sigmoid inhibitory effect model was used to describe a concentration-dependent inhibitory effect by diagnostic inhibitors and the various HIV PI:

$$E = E_{max} - \left[(E_{max} - E_0) \frac{C^{\gamma}}{C^{\gamma} + IC_{50}{}^{\gamma}} \right]$$

with E the accumulation of substrate in cells, E_{max} representing the accumulation of substrate without inhibitor, E_0 the accumulation of substrate at the maximum inhibitory effect of inhibitor, E_{max}-E_0 the maximum inhibitory effect, C the inhibitor concentration and γ the shape parameter (Hill coefficient). The best fits of the above equations to the individual accumulation data sets were obtained in Pharsight WinNonlin software v.5.2. (Pharsight, CA).

The Cheng–Prusoff equation (Cheng and Prusoff, 1973) was used to calculate the *Ki* from IC_{50}

values obtained in this study:

$$Ki = \frac{IC_{50}}{1 + \frac{S}{Km}}$$

where the IC_{50} is the concentration of the inhibitor producing a 50% inhibition, S is the substrate concentration under which the study is performed and Km is the Michaelis constant reflecting the affinity of the substrate (CGamF) for the transporter.

For comparison with the IC_{50} values obtained in transfected CHO cells, the IC_{50} values reflecting inhibition of CGamF accumulation in human hepatocytes were calculated from the data obtained previously (Ye et al., 2009), by linear regression of the Log(concentration) *versus* relative accumulation data.

Statistics. ANOVA (Dunnett) was used to evaluate statistical differences (SPSS v. 17.0 for Windows, SPSS Inc., Chicago (IL), USA). A p value of 0.01 was used as criterion for statistical significance.

Results:

Determination of CGamF accumulation kinetics in transfected CHO cells

Time-dependent cellular accumulation profiles for CGamF in OATP1B1 and OATP1B3 or wild-type CHO cells were determined for concentrations between 0.2 and 50 µM and initial accmulation rates were linear for the first 90 s of CGamF accumulation (data not shown). Initial net OATP1B1 or OATP1B3 mediated accumulation rates followed Michaelis-Menten kinetics. Average estimates for K_m and V_{max} are shown in Figure 1. CGamF exhibited an approximately 3-fold higher affinity and 5-fold higher V_{max} for OATP1B3 compared to OATP1B1.

Effect of diagnostic inhibitors and various HIV PI on CGamF accumulation in transfected CHO cells

To test whether known OATP inhibitors interact with OATP1B1 and 1B3-mediated CGamF accumulation, we quantified accumulation of 1 µM CGamF in the OATP1B1 and 1B3-expressing CHO cells in the absence and presence of different concentrations of rifampicin, digoxin and bromosulphophthalein and different HIV PI . The accumulation rate of 1 µM CGamF in OATP1B1 and 1B3-expressing CHO cells was linear up to 10 min. The results are summarized in Table 1 and Figure 2-3.

Rifampicin and bromosulphophthalein, known substrates/inhibitors of OATP1B1 and OATP1B3 (Vavricka et al., 2002; Annaert et al., 2007) were included as a positive control and inhibited almost completely the accumulation mediated by both OATPs with K_i values between 0.6 and 1.6 µM. Although the OATP1B3 substrate digoxin shows slight inhibiton of CGamF accumulation in OATP1B1-expressing CHO cells (K_i ~ 7 µM), it was 10-fold more potent in OATP1B3-expressing CHO cells with a K_i value of 0.7 µM. Digoxin did not completely block the transport of CGamF in

OATP1B3-expressing CHO cells.

Among the HIV PI tested, all except nelfinavir show a concentration-dependent inhibitory effect on CGamF accumulation by both OATP isoforms. Table 1 compares the IC_{50}/ K_i values of HIV PI for inhibition of OATP1B1 and 1B3-mediated CGamF (1 μM) accumulation with unbound plasma concentrations. Lopinavir is the most potent inhibitor with a K_i value around the unbound plasma concentration range. All other compounds exhibit K_i values above unbound plasma concentrations. The K_i values for the inhibiton by HIV PI in OATP1B1-expressing CHO cells correlated well with the values obtained in OATP1B3-expressing CHO cells (Figure 4A). The inhibitory effect of HIV PI on the CGamF accumulation in human hepatocytes has been investigated in a previous study (Ye et al., 2009). The IC_{50} values reflecting inhibition of CGamF accumulation by different HIV PI in human hepatocytes were estimated by linear regression of the Log(concentration) *versus* relative accumulation data. The corresponding K_i values were 0.1, 0.3, 5.8, 106, 123 and 219 μM for atazanavir, darunavir, indinavir, saquinavir, ritonavir, and amprenavir, respectively. Apart from saquinavir and ritonavir, some correlation could be discerned between K_i values in human hepatocytes and those obtained in OATP1B1- or OATP1B3- expressing CHO cells (Figure 4 B, C).

CGamF and E3S accumulation in Caco-2 cells.

Transporter expression profiling of the Caco-2 cell populations used in our lab along with those obtained from other labs revealed that our Caco-2 cells (as well as those of most other labs tested) express high levels of OATP2B1 with absent or very low levels of the other OATP isoforms (Hayeshi et al., 2008). Previous work has shown that OATP2B1 is predominantly responsible for the apical accumulation of E3S in Caco-2 cells (Sai et al., 2006). In the present study, the accumulation activity of OATP2B1 using E3S as substrate showed highest in week 2 Caco-2

cultures. No accumulation of CGamF could be detected in Caco-2 cells, indicating that CGamF is most likely a very poor OATP2B1 substrate.

In order to study the inhibitory effects of HIV PI on OATP2B1 activity, E3S was used as probe substrate. Initial accumulation of E3S across the apical membrane of Caco-2 cells was determined at 2 min. Biphasic saturation kinetics were observed consistent with results from a previous study (Sai et al., 2006). The K_m values of the high- and low-affinity sites were 3.2 ± 0.3 μM and 2.9 ± 0.1 mM, and V_{max} values were 41.1 ± 3.2 pmol/mg protein/2 min and 7.9 ± 0.5 nmol/mg protein/2 min, respectively (Figure 5, A B). By comparing the values of the V_{max}/K_m ratio for high- and low-affinity sites, the contribution of the high-affinity site to overall accumulation clearance at low concentration was estimated to be approximately 4 times larger than that of the low-affinity site.

Effect of OATP inhibitors and various HIV PIs on E3S accumulation in Caco-2 cells

The known OATP inhibitors, rifampicin, rifamycin SV, bromosulphophthalein and E3S itself significantly inhibited E3S accumulation in Caco-2 cells, while the specific OATP1B3 substrate digoxin had no effect. Among eight tested HIV PI, indinavir, ritonavir and saquinavir showed the most potent inhibition of E3S accumulation in Caco-2 cells (Figure 6).

For the four OATP inhibitors and the three most potent HIV PI, concentration-dependent inhibitory effect on the E3S accumulation in Caco-2 cells were studied in more detail (Figure 7). E3S accumulation in Caco-2 cells was strongly inhibited by the sulfate conjugate bromosulphophthalein (Table 2), yielding an IC_{50} value comparable with the reported value (2.9 μM) (Sai et al., 2006). The IC_{50}/K_i values for ritonavir, saquinavir and indinavir were all above the unbound plasma concentration reported for these HIV PI (see Table 1).

Discussion

In the present study, we first investigated the relative roles of the three different human hepatic OATP isoforms in CGamF accumulation. Relatively high CGamF accumulation rates were observed in OATP1B1- and OATP1B3-transfected CHO cells (Figure 1), yielding accumulation clearance values (V_{max}/K_m) of 7.8 and 142 µl/min/mg protein, respectively. For comparison, reported values (Treiber et al., 2007; Gui et al., 2008) for accumulation of previously tested OATP1B1 and 1B3 substrates in these transfected cells are: 30 and 23 µl/min/mg protein for bosentan, 67 and 23 µl/min/mg protein for estradiol-17β-D-glucuronide, 142 and 32 µl/min/mg protein for E3S, and 0.034 and 0.203 µl/min/mg protein for Fluo-3. This allows categorizing CGamF as an excellent substrate for the OATP1B transporter subfamily. In contrast, no accumulation of CGamF could be detected in Caco-2 monolayers, indicating that OATP2B1, by far the most abundant transporter among the OATPs expressed in this cell line (Sai et al., 2006; Hayeshi et al., 2008), is not mediating CGamF accumulation to any appreciable extent. Assuming that the transport behaviour of CGamF is mainly determined by its bile salt moiety, the latter finding is consistent with previous reports stating that OATP2B1, in contrast to the 1B1 and 1B3 isoforms, does not mediate bile acid transport (Kullak-Ublick et al., 2001). Along with our previous *in vitro* data on CGamF accumulation in human hepatocytes, demonstrating significant inhibition of sodium-independent CGamF accumulation by the OATP inhibitor rifampicin (as well as various HIV PI) (Ye et al., 2009), OATP1B3 appears to be the main sodium-independent transporter mediating human hepatic CGamF accumulation. In addition, incubations with human hepatocytes in the absence of sodium had implied NTCP supporting about 36 % of active CGamF accumulation (Ye et al., 2009). Although the combination of *in vitro* data thus far obtained for CGamF (in human hepatocytes and transfected systems) do not allow to completely exclude a role for other

sodium-independent mechanisms (e.g. OAT2; *SLC22A7*) mediating hepatic CGamF accumulation, the fact that CGamF is an amphiphilic bile acid analogue provides further evidence for the key role of OATP transporters, *in casu* the 1B3 isoform. Even though the relative expression level of OATP1B1 is about 2-fold higher than OATP1B3 in human liver (Hilgendorf et al., 2007), these data support the use of CGamF as an *in vitro* probe substrate for sodium-independent substrate accumulation in human hepatocytes essentially mediated by OATP1B3.

Interference with OATP1B1 and 1B3-mediated CGamF accumulation was studied for the diagnostic OATP inhibitors/substrates rifampicin, digoxin and bromosulphophtalein, as well as for most HIV PI in clinical use today (Table 1; Figure 1-2). The inhibition by rifampicin and bromosulphophthalein is comparable for both OATP isoforms (K_i values between 0.6 and 1.6 μM), whereas upon coincubation with digoxin a much higher potency was observed for inhibiting OATP1B3 (K_i = 0.7 μM) compared to OATP1B1 (K_i = 7 μM). The observation that digoxin affected OATP1B1-mediated accumulation, albeit at a lower potency than for OATP1B3, is remarkable in light of reports classifying digoxin as a specific OATP1B3 substrate (Kullak-Ublick et al., 2001). However, its specificity as an inhibitor was not tested in the latter study and weak interference of digoxin with OATP1B1-mediated pitavastatin accumulation has also been reported (K_i=32 μM) (Hirano et al., 2006). It should be emphasized that the latter observation as well as our present data do not imply that OATP1B1 mediates digoxin transport, but only indicate some affinity of digoxin for OATP1B1. Digoxin accumulation in transfected oocytes has indeed been shown for OATP1B3 only, and not for the 1B1, 2B1 or 1A2 isoforms (Kullak-Ublick et al., 2001). It is also noteworthy that digoxin showed relatively poor efficacy for inhibition of CGamF accumulation by both OATP1B isoforms (38% - 54% max inhibition), which may indicate that multiple binding sites are involved. Using estradiol-17β-D-glucuronide as a substrate and/or inhibitor, multiple binding

sites on rat Oatp1a4 have been suggested to explain activation as well as inhibition of Oatp-mediated substrate accumulation in hepatocytes (Sugiyama et al., 2002; Annaert and Brouwer, 2005).

The concentration-dependent inhibition curves (Figure 2-3) for the various HIV PI with respect to CGamF accumulation in OATP1B1- and OATP1B3-expressing CHO cells illustrate that most HIV PI exhibit significant affinity for the OATP1B transporter subfamily. K_i values covered a rather broad range (Table 1; Figure 4A), between 0.5 and 12.8 μM for OATP1B1 inhibition and between 1.4 and 13.1 μM for OATP1B3 inhibition. As compared to the other HIV PI tested, lopinavir was remarkably potent for inhibiting OATP1B-mediated CGamF accumulation. With K_i values all within the 1.4 - 3.3 μM range, the inhibiting potencies of saquinavir, ritonavir, atazanavir and darunavir were very similar, whereas much higher K_i values were observed for indinavir and amprenavir (8.5-13 μM). The remarkably potent effect of lopinavir is certainly of interest in light of results from a clinical drug interaction study including lopinavir/ritonavir and the OATP substrate fexofenadine (van Heeswijk et al., 2006). In this article, the authors had speculated about the possible interference of transporters different from P-glycoprotein, such as OATPs, to explain the increased fexofenadine plasma levels. In another study, coadministration of rosuvastatin and lopinavir/ritonavir in healthy volunteers was associated with an approximately 2- and 5-fold increase in rosuvastatin steady-state AUC and C_{max}, respectively (Kiser et al., 2008). This increase was considered to be clinically significant requiring dose adjustment and this drug interaction was suggested to be mediated via inhibition of OATP1B1 by either ritonavir and/or lopinavir (Ayrton and Morgan, 2008). Our *in vitro* data appear to support inhibition of OATP1B1 by lopinavir (rather than ritonavir) as a major mechanism here, since the unbound plasma C_{max} level for lopinavir (0.3 μM) is only slightly lower than the K_i value in our *in vitro* system.

Figure 4A illustrates that there is a rather good correlation between inhibition potencies of both isoforms, which may indicate binding to corresponding sites on both isoforms. This is not surprising given the 80% amino acid identity between the 1B1 and 1B3 isoforms (Hagenbuch and Meier, 2003). In the present study, the most pronounced difference between both isoforms in terms of inhibiting potency was observed for lopinavir with a 3-fold higher affinity for OATP1B1 compared to OATP1B3. For all other HIV PI, the difference was less than 2-fold. Nevertheless, considering the unbound C_{max} concentration of lopinavir (0.3 μM), the difference in potency for lopinavir towards both isoforms may be critical with respect to the clinical relevance of drug interactions occurring at the level of OATP1B1 versus OATP1B3. In light of the above mentioned clinically relevant drug interaction between fexofenadine and lopinavir/ritonavir, inhibition of OATP1B1 by lopinavir would be the most likely mechanism. However, the relative contribution of multiple OATP isoforms to fexofenadine disposition remains controversial. Shimizu et al. (Shimizu et al., 2005) have demonstrated that OATP1B3 contributes mainly to the hepatic accumulation of fexofenadine using transporter-expressing HEK293 cells. On the other hand, Niemi et al. (Niemi et al., 2005) reported that the genetic polymorphism of OATP1B1 (T521C), which was been shown to decrease the transport clearance, increased the plasma AUC of fexofenadine. These results suggested that OATP1B1 as well as OATP1B3 are involved in the accumulation of fexofenadine into human liver. The exact relative roles of both isoforms in the drug interaction between fexofenadine and lopinavir/ritonavir remain to be elucidated.

As mentioned before, in contrast to the efficient accumulation of CGamF by the human OATP1B isoforms, no accumulation of CGamF could be detected in Caco-2 cells. As virtually exclusive expression of the 2B1 isoform among multiple members of the OATP family was shown in the Caco-2 clone used in the present study (Hayeshi and others 2008), any role for OATP2B1 in

the disposition of CGamF in human liver is highly unlikely. However, consistent with previous reports, efficient accumulation of E3S was observed across the apical membrane of Caco-2 cells, thus enabling the use of this cell line as a surrogate in vitro tool for hepatic OATP2B1-mediated substrate accumulation. Based on observed kinetics for E3S (Figure 5), accumulation clearance values of 1.4 and 6.4 µl/min/mg protein were obtained for the low and high capacity components, respectively. As illustrated in Figure 6, the low affinity of digoxin for the OATP2B1 isoform was confirmed with no effect on E3S accumulation. In contrast, the less specific and/or more potent OATP inhibitors bromosulphophthalein , rifamycin SV and rifampicin all significantly reduced E3S accumumation. Among the HIV PI tested at high concentrations (10-50 µM; Figure 6), only indinavir, ritonavir and saquinavir exhibited significant effects. However, with K_i values between 3.0 and 4.8 µM (Table 2, Figure 6), these PI were less potent compared to typical OATP inhibitors (K_i = 1.5-2.3 µM).

Since interaction studies for OATP2B1 were necessarily conducted with E3S instead of CGamF as substrate, comparison of inhibitory effects of HIV PI on 2B1 with the effects of HIV PI on OATP1B1 and 1B3-mediated CGamF accumulation should occur with caution; the inhibitory effects will be substrate-dependent. Nevertheless, it appears that only ritonavir and saquinavir exhibited comparable potency for inhibition of all OATP isoforms tested. Indeed, the potent effects of lopinavir on the OATP1B subfamily was not observed for OATP2B1, while indinavir as the most potent OATP2B1 inhibitor (K_i =3 µM) among the HIV PI, was about 3-fold less potent against OATP1B-mediated CGamF accumulation.

Comparison of the effects of these HIV PI on CGamF accumulation between human hepatocytes and OATP1B-transfected CHO cells (Figure 4B,C) reveals some relationship for atazanavir, darunavir, indinavir and amprenavir. However, much higher K_i values were obtained for

ritonavir and saquinavir in human hepatocytes compared to OATP1B1 and 1B3-transfected CHO cells. This discrepancy may be explained in different ways. One explanation for this observation may be that sinusoidal efflux mechanisms (e.g. *ABCC3*; MRP3) present in human hepatocytes but not in transfected CHO cells limit the intracellular concentrations of saquinavir and ritonavir to a larger extent compared to other PI. However, this would imply binding that these PI inhibit OATP1B by binding to its intracellular domain, while to date no evidence has been reported for OATP inhibition from the cytoplasmic side. Alternatively, it should be noted that inhibition of active CGamF accumulation in human hepatocytes (Ye et al., 2009) was studied under conditions supporting contribution of both sodium-independent (OATP-mediated) as well as sodium dependent (NTCP-mediated; 35%) pathways. The relatively higher concentrations which may be needed to inhibit NTCP-mediated CGamF transport by saquinavir and ritonavir, may exlain the higher K_i values in hepatocytes compared to OATP1B1 and 1B3-transfected cells. However, even when using taurocholate as the prototypical NTCP substrate, both ritonavir and saquinavir were shown to be relatively potent inhibitors (IC_{50} = 2.1 and 6.7 μM) of human NTCP (McRae et al., 2006). It will be necessary to also study the effects of the various HIV PI on NTCP-mediated CGamF transport in order to gain a better understanding of the inhibition profiles observed in human hepatocytes.

In conclusion, we have obtained *in vitro* data illustrating isoform-specific interaction of HIV PI with the OATP family of human hepatic transporters. The interaction profiles obtained in cells transfected with a single OATP1B isoform correlated only partly with the interaction profiles obtained in human hepatocytes. Lopinavir was shown to be remarkably potent in inhibiting OATP1B1 (and to a lesser extent OATP1B3) and this inhibition may explain clinically relevant drug interactions involving drugs (e.g. fexofenadine) relying on OATPs for their hepatobiliary

elimination. Although a different substrate had to be used to study OATP2B1 interaction, HIV PI displayed completely different interaction profiles for this isoform compared to the OATP1B subfamily. Generating drug interaction profiles in various *in vitro* systems, including human hepatocytes and transfected cells, will ultimately contribute to a better understanding of the mechanisms underlying clinically relevant drug interactions.

Acknowledgements

This work was supported by a grant from the Fonds voor Wetenschappelijk Onderzoek (FWO Vlaanderen). Z-W Ye is recipient of an SBA-China Scholarship from the Katholieke Universiteit Leuven.

Declaration of interest

The authors report no declaration of interest.

References

Annaert PP and Brouwer KL (2005) Assessment of drug interactions in hepatobiliary transport using rhodamine 123 in sandwich-cultured rat hepatocytes. *Drug Metab Dispos* 33:388-394.

Annaert PP, Swift B, Lee JK and Brouer KLR (2007) Drug Transporters: Molecular Characterization and Role in Drug Disposition, in: *Drug Transport in the Liver* (You G and Morris M eds), John Wiley &Sons, Inc., New York.

Ayrton A and Morgan P (2008) Role of transport proteins in drug discovery and development: a pharmaceutical perspective. *Xenobiotica* 38:676-708.

Bravo P, Bender V and Cassio D (1998) Efficient in vitro vectorial transport of a fluorescent conjugated bile acid analogue by polarized hepatic hybrid WIF-B and WIF-B9 cells. *Hepatology* 27:576-583.

Chandwani A and Shuter J (2008) Lopinavir/ritonavir in the treatment of HIV-1 infection: a review. *Ther Clin Risk Manag* 4:1023-1033.

Cheng Y and Prusoff WH (1973) Relationship between the inhibition constant (K1) and the concentration of inhibitor which causes 50 per cent inhibition (I50) of an enzymatic reaction. *Biochem Pharmacol* 22:3099-3108.

Cooper KJ, Martin PD, Dane AL, Warwick MJ, Raza A and Schneck DW (2003) Lack of effect of ketoconazole on the pharmacokinetics of rosuvastatin in healthy subjects. *Br J Clin Pharmacol* 55:94-99.

de Bruin M, Miyake K, Litman T, Robey R and Bates SE (1999) Reversal of resistance by GF120918 in cell lines expressing the ABC half-transporter, MXR. *Cancer Lett* 146:117-126.

DuBuske LM (2005) The role of P-glycoprotein and organic anion-transporting polypeptides in drug interactions. *Drug Saf* 28:789-801.

Endres CJ, Hsiao P, Chung FS and Unadkat JD (2006) The role of transporters in drug interactions. *Eur J Pharm Sci* 27:501-517.

Gekeler V, Ise W, Sanders KH, Ulrich WR and Beck J (1995) The leukotriene LTD4 receptor antagonist MK571 specifically modulates MRP associated multidrug resistance. ***Biochem Biophys Res Commun*** **208:345-352.**

Gui C, Miao Y, Thompson L, Wahlgren B, Mock M, Stieger B and Hagenbuch B (2008) Effect of pregnane X receptor ligands on transport mediated by human OATP1B1 and OATP1B3. ***Eur J Pharmacol*** **584:57-65.**

Hagenbuch B and Gui C (2008) Xenobiotic transporters of the human organic anion transporting polypeptides (OATP) family. ***Xenobiotica*** **38:778-801.**

Hagenbuch B and Meier PJ (2003) The superfamily of organic anion transporting polypeptides. ***Biochim Biophys Acta*** **1609:1-18.**

Hagenbuch B, Scharschmidt BF and Meier PJ (1996) Effect of antisense oligonucleotides on the expression of hepatocellular bile acid and organic anion uptake systems in Xenopus laevis oocytes, pp 901-904.

Hayeshi R, Hilgendorf C, Artursson P, Augustijns P, Brodin B, Dehertogh P, Fisher K, Fossati L, Hovenkamp E, Korjamo T, Masungi C, Maubon N, Mols R, Mullertz A, Monkkonen J, O'Driscoll C, Oppers-Tiemissen HM, Ragnarsson EG, Rooseboom M and Ungell AL (2008) Comparison of drug transporter gene expression and functionality in Caco-2 cells from 10 different laboratories. ***Eur J Pharm Sci*** **35:383-396.**

Hilgendorf C, Ahlin G, Seithel A, Artursson P, Ungell AL and Karlsson J (2007) Expression of thirty-six drug transporter genes in human intestine, liver, kidney, and organotypic cell lines. ***Drug Metab Dispos*** **35:1333-1340.**

Hirano M, Maeda K, Shitara Y and Sugiyama Y (2006) Drug-drug interaction between pitavastatin and various drugs via OATP1B1. ***Drug Metab Dispos*** **34:1229-1236.**

Hoetelmans R VdSI, Pauw MD, Struble K, Peeters M, Van der Geest R. (2003) TMC114, A Next Generation HIV Protease Inhibitor: Pharmacokinetics and Safety Following Oral Administration of Multiple Doses

With and Without Low Doses of Ritonavir in Healthy Volunteers., in: ***10th Conference on Retroviruses and Opportunistic Infections*****, Boston (MA).**

Holzinger F, Schteingart CD, Ton-Nu HT, Cerre C, Steinbach JH, Yeh HZ and Hofmann AF (1998) Transport of fluorescent bile acids by the isolated perfused rat liver: kinetics, sequestration, and mobilization. ***Hepatology*** **28:510-520.**

Huang L, Wang Y and Grimm S (2006) ATP-dependent transport of rosuvastatin in membrane vesicles expressing breast cancer resistance protein. ***Drug Metab Dispos*** **34:738-742.**

Kiser JJ, Gerber JG, Predhomme JA, Wolfe P, Flynn DM and Hoody DW (2008) Drug/Drug interaction between lopinavir/ritonavir and rosuvastatin in healthy volunteers. ***J Acquir Immune Defic Syndr*** **47:570-578.**

Konig J, Seithel A, Gradhand U and Fromm MF (2006) Pharmacogenomics of human OATP transporters. ***Naunyn Schmiedebergs Arch Pharmacol*** **372:432-443.**

Kullak-Ublick GA, Ismair MG, Stieger B, Landmann L, Huber R, Pizzagalli F, Fattinger K, Meier PJ and Hagenbuch B (2001) Organic anion-transporting polypeptide B (OATP-B) and its functional comparison with three other OATPs of human liver. ***Gastroenterology*** **120:525-533.**

Letschert K, Faulstich H, Keller D and Keppler D (2006) Molecular characterization and inhibition of amanitin uptake into human hepatocytes. ***Toxicol Sci*** **91:140-149.**

Link E, Parish S, Armitage J, Bowman L, Heath S, Matsuda F, Gut I, Lathrop M and Collins R (2008) SLCO1B1 variants and statin-induced myopathy--a genomewide study. ***N Engl J Med*** **359:789-799.**

Maglova LM, Jackson AM, Meng XJ, Carruth MW, Schteingart CD, Ton-Nu HT, Hofmann AF and Weinman SA (1995) Transport characteristics of three fluorescent conjugated bile acid analogs in isolated rat hepatocytes and couplets. ***Hepatology*** **22:637-647.**

Marin-Niebla A, Lopez-Cortes LF, Ruiz-Valderas R, Viciana P, Mata R, Gutierrez A, Pascual R and Rodriguez

M (2007) Clinical and pharmacokinetic data support once-daily low-dose boosted saquinavir (1,200 milligrams saquinavir with 100 milligrams ritonavir) in treatment-naive or limited protease inhibitor-experienced human immunodeficiency virus-infected patients. *Antimicrob Agents Chemother* 51:2035-2042.

McRae MP, Lowe CM, Tian X, Bourdet DL, Ho RH, Leake BF, Kim RB, Brouwer KL and Kashuba AD (2006) Ritonavir, saquinavir, and efavirenz, but not nevirapine, inhibit bile acid transport in human and rat hepatocytes. *J Pharmacol Exp Ther* 318:1068-1075.

Mita S, Suzuki H, Akita H, Hayashi H, Onuki R, Hofmann AF and Sugiyama Y (2006) Inhibition of bile acid transport across Na+/taurocholate cotransporting polypeptide (SLC10A1) and bile salt export pump (ABCB 11)-coexpressing LLC-PK1 cells by cholestasis-inducing drugs. *Drug Metab Dispos* 34:1575-1581.

Niemi M, Kivisto KT, Hofmann U, Schwab M, Eichelbaum M and Fromm MF (2005) Fexofenadine pharmacokinetics are associated with a polymorphism of the SLCO1B1 gene (encoding OATP1B1). *Br J Clin Pharmacol* 59:602-604.

Noe J, Portmann R, Brun ME and Funk C (2007) Substrate-dependent drug-drug interactions between gemfibrozil, fluvastatin and other organic anion-transporting peptide (OATP) substrates on OATP1B1, OATP2B1, and OATP1B3. *Drug Metab Dispos* 35:1308-1314.

Perry CM, Frampton JE, McCormack PL, Siddiqui MA and Cvetkovic RS (2005) Nelfinavir: a review of its use in the management of HIV infection. *Drugs* 65:2209-2244.

Ruane PJ, Luber AD, Wire MB, Lou Y, Shelton MJ, Lancaster CT and Pappa KA (2007) Plasma amprenavir pharmacokinetics and tolerability following administration of 1,400 milligrams of fosamprenavir once daily in combination with either 100 or 200 milligrams of ritonavir in healthy volunteers. *Antimicrob Agents Chemother* 51:560-565.

Sai Y, Kaneko Y, Ito S, Mitsuoka K, Kato Y, Tamai I, Artursson P and Tsuji A (2006) Predominant contribution of organic anion transporting polypeptide OATP-B (OATP2B1) to apical uptake of estrone-3-sulfate by human intestinal Caco-2 cells. ***Drug Metab Dispos*** **34:1423-1431.**

Shimizu M, Fuse K, Okudaira K, Nishigaki R, Maeda K, Kusuhara H and Sugiyama Y (2005) Contribution of OATP (organic anion-transporting polypeptide) family transporters to the hepatic uptake of fexofenadine in humans. ***Drug Metab Dispos*** **33:1477-1481.**

Shitara Y, Horie T and Sugiyama Y (2006) Transporters as a determinant of drug clearance and tissue distribution. ***European Journal of Pharmaceutical Sciences*** **27:425-446.**

Simonson SG, Raza A, Martin PD, Mitchell PD, Jarcho JA, Brown CD, Windass AS and Schneck DW (2004) Rosuvastatin pharmacokinetics in heart transplant recipients administered an antirejection regimen including cyclosporine. ***Clin Pharmacol Ther*** **76:167-177.**

Soars MG, McGinnity DF, Grime K and Riley RJ (2007) The pivotal role of hepatocytes in drug discovery. ***Chem Biol Interact*** **168:2-15.**

Sugiyama D, Kusuhara H, Shitara Y, Abe T and Sugiyama Y (2002) Effect of 17 beta-estradiol-D-17 beta-glucuronide on the rat organic anion transporting polypeptide 2-mediated transport differs depending on substrates. ***Drug Metab Dispos*** **30:220-223.**

Swainston Harrison T and Scott LJ (2005) Atazanavir: a review of its use in the management of HIV infection. ***Drugs*** **65:2309-2336.**

Tamai I, Nozawa T, Koshida M, Nezu J, Sai Y and Tsuji A (2001) Functional characterization of human organic anion transporting polypeptide B (OATP-B) in comparison with liver-specific OATP-C. ***Pharm Res*** **18:1262-1269.**

Treiber A, Schneiter R, Hausler S and Stieger B (2007) Bosentan is a substrate of human OATP1B1 and OATP1B3: inhibition of hepatic uptake as the common mechanism of its interactions with cyclosporin A,

rifampicin, and sildenafil. *Drug Metab Dispos* 35:1400-1407.

van Heeswijk RP, Bourbeau M, Campbell P, Seguin I, Chauhan BM, Foster BC and Cameron DW (2006) Time-dependent interaction between lopinavir/ritonavir and fexofenadine. *J Clin Pharmacol* 46:758-767.

Vavricka SR, Van Montfoort J, Ha HR, Meier PJ and Fattinger K (2002) Interactions of rifamycin SV and rifampicin with organic anion uptake systems of human liver. *Hepatology* 36:164-172.

Wallstab A, Koester M, Bohme M and Keppler D (1999) Selective inhibition of MDR1 P-glycoprotein-mediated transport by the acridone carboxamide derivative GG918. *Br J Cancer* 79:1053-1060.

Wang Q, Strab R, Kardos P, Ferguson C, Li J, Owen A and Hidalgo IJ (2008) Application and limitation of inhibitors in drug-transporter interactions studies. *International Journal of Pharmaceutics* 356:12-18.

Williams GC and Sinko PJ (1999) Oral absorption of the HIV protease inhibitors: a current update. *Adv Drug Deliv Rev* 39:211-238.

Xiang X, han Y, Neuvonen M, Pasanen Mk, kalliokoski A, Backman JT, laitila J, Neuvonen PJ and Niemi M (2009) Effect of SLCO1B1 polymorphism on plasma bile acid. *Drug Metab Rev.* 41:A167.

Yamazaki M, Li B, Louie SW, Pudvah NT, Stocco R, Wong W, Abramovitz M, Demartis A, Laufer R, Hochman JH, Prueksaritanont T and Lin JH (2005) Effects of fibrates on human organic anion-transporting polypeptide 1B1-, multidrug resistance protein 2- and P-glycoprotein-mediated transport. *Xenobiotica* 35:737-753.

Ye ZW, Augustijns P and Annaert P (2008) Cellular accumulation of cholyl-glycylamido-fluorescein in sandwich-cultured rat hepatocytes: kinetic characterization, transport mechanisms, and effect of human immunodeficiency virus protease inhibitors. *Drug Metab Dispos* 36:1315-1321.

Ye ZW, van Pelt J, Camus S, Snoeys J, Augustijns P and Annaert P (2009) Species-specific interaction of HIV protease inhibitors with accumulation of cholyl-glycylamido-fluorescein (CGamF) in sandwich-cultured hepatocytes. *J. Pharm Sci*:In press.

Table 1. Comparison of IC_{50} and K_i values of HIV PI for inhibition of OATP1B1 and 1B3-mediated CGamF (1 µM) accumulation with unbound plasma concentrations, IC_{50} values were calculated according to the sigmoid inhibitory effect model as described in the Methods section.

Inhibitors	Maxium inhibition (% of control)		IC_{50} (µM)		Ki (µM)		Plasma protein binding*	C_{max} corrected for plasma protein binding (µM)*
	OATP1B1	OATP1B3	OATP1B1	OATP1B3	OATP1B1	OATP1B3		
amprenavir	61 ±9	75 ± 2	14.4 ± 3.8	19.1 ± 2.0	12.8	13.1	90%	1.0-3.2
atazanavir	72 ± 8	87 ± 7	1.7 ± 0.2	3.0 ± 1.0	1.5	2.0	86%	0.6-1.3
darunavir	66 ± 3	83 ± 2	3.5 ± 1.1	4.8 ± 0.8	3.1	3.3	93%	0.3-1.1
indinavir	63 ± 4	76 ± 2	12.2 ± 4.2	12.3 ± 1.1	10.8	8.5	65%	1.7-4.4
lopinavir	76 ± 3	89 ± 2	0.5 ± 0.1	2.0 ± 0.1	0.5	1.4	98%	0.3
nelfinavir**	38 ± 9	34 ± 6	ND	ND	ND	ND	98%	0.10
ritonavir	73 ± 1	86 ± 4	1.6 ± 0.3	3.6 ± 1.1	1.4	2.5	99%	0.16
saquinavir	74 ± 0.3	80 ± 4	2.1 ± 1.2	4.1 ± 1.0	1,8	2.8	98%	0.11-0.30
rifampicin	79 ± 5	94 ± 3	1.8 ± 0.3	1.3 ± 0.7	1.6	0.9	-	-
digoxin	38 ± 7	54 ± 9	7.9 ± 2.1	1.0 ± 0.4	7.0	0.7	-	-
bromosulphophthalein	74 ± 9	92 ± 3	0.7 ± 0.4	1.4 ± 0.4	0.6	1.0	-	-

ND: Not determined.

*: from (Williams and Sinko, 1999; Hoetelmans R, 2003; Perry et al., 2005; Swainston Harrison and Scott, 2005; Marin-Niebla et al., 2007; Ruane et al., 2007; Chandwani and Shuter, 2008)

**: due to solubility limitations, nelfinavir could only be tested up to a concentration of 20 µM

Table 2. IC_{50} and K_i values of human OATP inhibitors and various HIV PI for inhibition of OATP2B1 mediated E3S (1 μM) accumulation across the apical membrane of Caco-2 monolayers, IC_{50} and K_i values were calculated as described in the Methods section.

Inhibitors	IC_{50} (μM)	Ki (μM)
Bromosulfophthalein	2.0 ± 0.5	1.5
Rifampicin	2.1 ± 1.5	1.6
Estrone-3-sulfate	2.5 ± 0.9	1.9
Rifymicin SV	3.0 ± 1.1	2.3
Indinavir	3.9 ± 0.6	3.0
Saquinavir	5.3 ± 1.3	4.0
Ritonavir	6.3 ± 2.9	4.8

Figure Legends

Figure 1. Concentration-dependent net accumulation of CGamF in OATP1B1- (panel A) and OATP1B3- (panel B) expressing CHO cells. Net accumulation values were obtained by subtracting accumulation in wild-type CHO cells from total accumulation in transfected cells. Points represent mean (± S.D.) of triplicate measurements. Solid lines were obtained by fitting the Michaelis-Menten equation to the experimental data by using the Solver tool in Microsoft Excel 2003.

Figure 2. Concentration dependent inhibition of CGamF accumulation in OATP1B1-expressing CHO cells. Accumulation of 1μM CGamF was measured at 37 °C for 10 min in OATP1B1-expressing and wild type CHO cells in the absence or presence of different concentrations of rifampicin, digoxin, bromosulphophthalein and various HIV PI. Net accumulation values were obtained by subtracting accumulation in wild-type CHO cells from total accumulation in transfected cells. Points represent mean (± S.D.) of triplicate measurements. Lines represent best fit to the data according to the sigmoid inhibitory effect model as described in the Methods section.

Figure 3. Concentration dependent inhibition of CGamF accumulation in OATP1B3-expressing CHO cells. Accumulation of 1μM CGamF was measured at 37 °C for 10 min in OATP1B3-expressing and wild type CHO cells in the absence or presence of different concentrations of rifampicin, digoxin, bromosulphophthalein and various HIV PI. Net accumulation values were obtained by subtracting accumulation in wild-type CHO cells from total accumulation in transfected cells. Points represent mean (± S.D.) of triplicate measurements. Lines represent best fit to the data according to the sigmoid inhibitory effect model as described in the Methods section.

Figure 4. Relationship between K_i values obtained in OATP1B1-expressing CHO cells and OATP1B3-expressing CHO cells (A); and between K_i values obtained using human hepatocytes (Ye et al., 2009) *versus* OATP1B1-expressing CHO cells (B) or *versus* OATP1B3-expressing CHO cells (C).

Figure 5. Concentration dependent accumulation of E3S in Caco-2 cells. Points represent mean (± S.D.) of triplicate measurements. Dotted and solid lines represent the saturable and nonsaturable accumulation obtained by a model incorporating both a two phase Michaelis-Menten (saturable) and a linear (non-saturable) component (A). Saturable accumulation of E3S is also shown as an Eadie-Hofstee plot (B).

Figure 6. Effect of different inhibitors on the accumulation of E3S in Caco-2 cells. Each bar represents mean (± S.D.) relative to control accumulation as function of different inhibitors. **, $p<0.01$ (ANOVA, Dunnet), compared to the control accumulation.

Figure 7. Concentration-dependent inhibition of E3S (1 μM) accumulation (10 min, 37 °C) across the apical membrane of Caco-2 monolayers. Points represents the mean (± S.D.) relative to control accumulation as function of different concentrations of rifampicin, rifamycin SV, bromosulphophthalein, estrone-3-sulfate and various HIV PI. Lines represent best fit to the data according to the sigmoid inhibitory effect model as described in the Methods section.

Figure 1

A

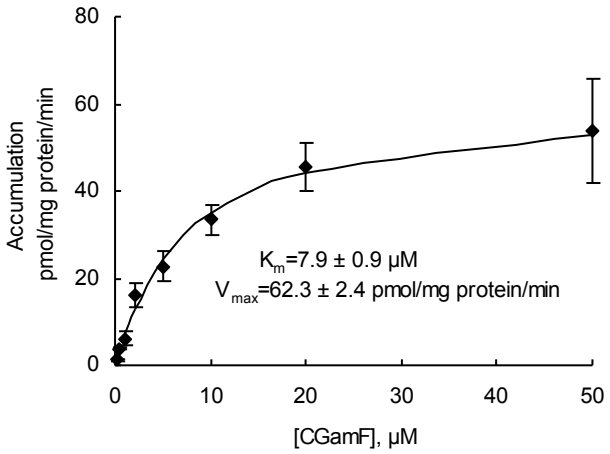

B

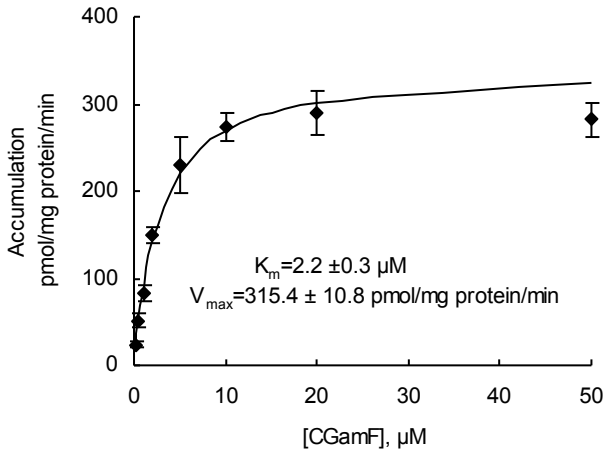

Figure 2

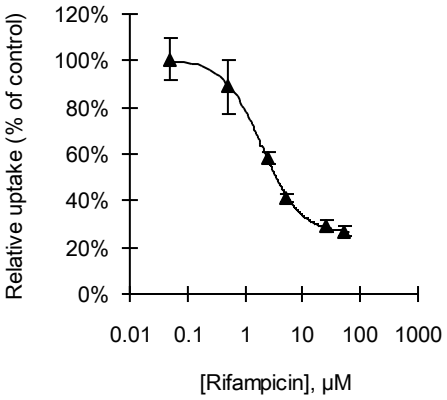

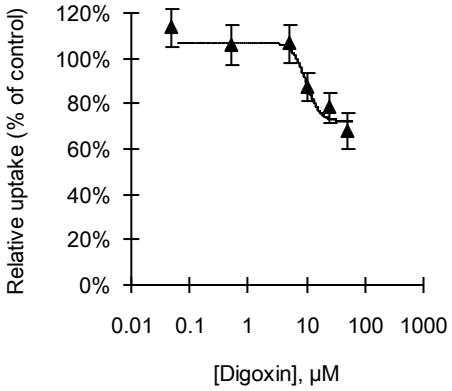

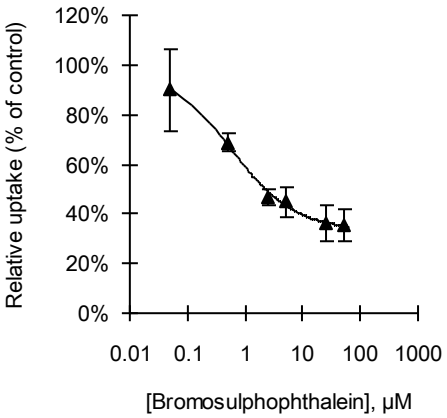

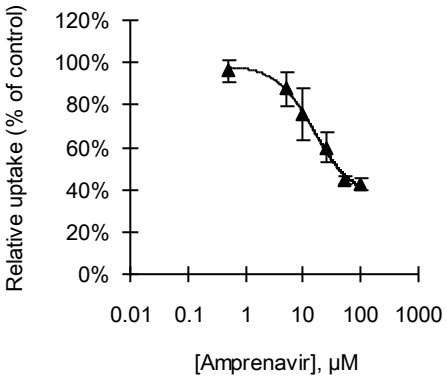

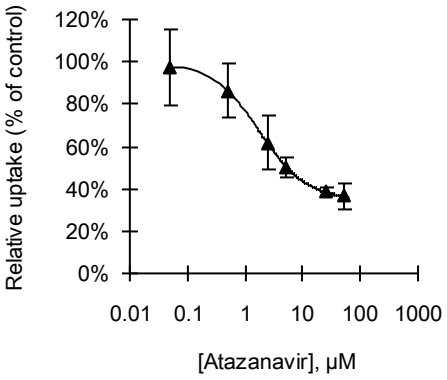

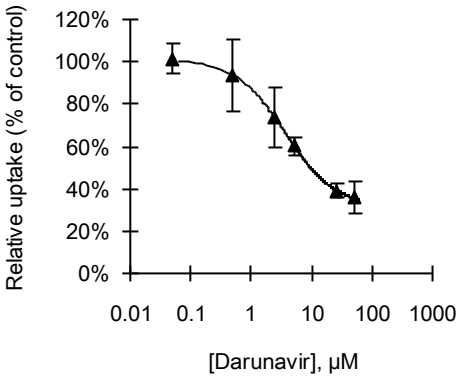

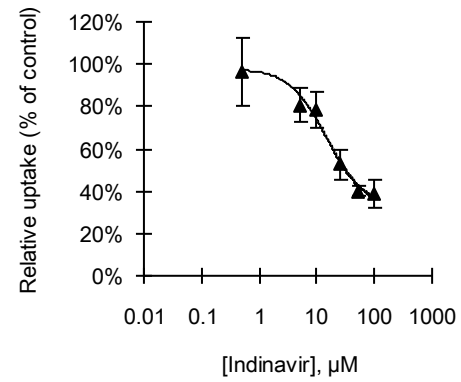
Relative uptake (% of control)
120%
100%
80%
60%
40%
20%
0%
0.01
0.1
1
10
100
1000
[Indinavir], µM

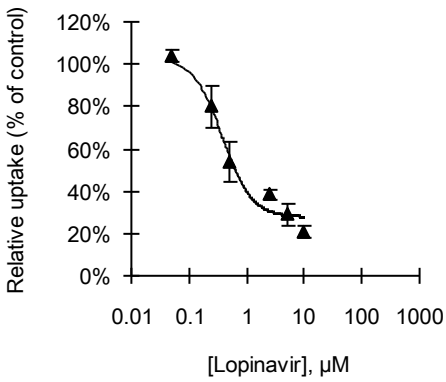
Relative uptake (% of control)
120%
100%
80%
60%
40%
20%
0%
0.01
0.1
1
10
100
1000
[Lopinavir], µM

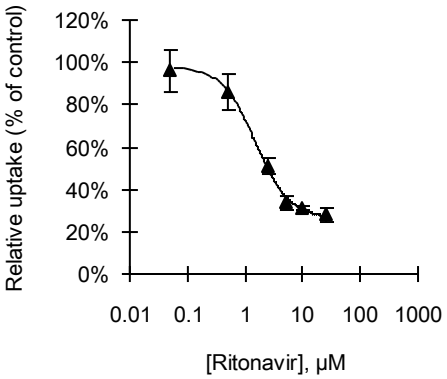
Relative uptake (% of control)
120%
100%
80%
60%
40%
20%
0%
0.01
0.1
1
10
100
1000
[Ritonavir], µM

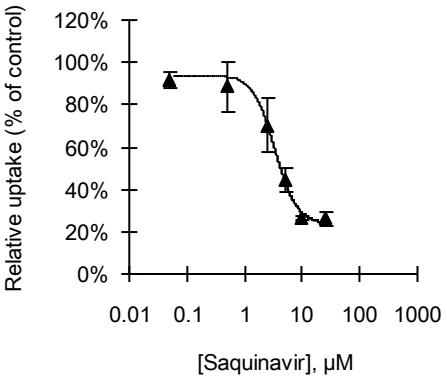
Relative uptake (% of control)
120%
100%
80%
60%
40%
20%
0%
0.01
0.1
1
10
100
1000
[Saquinavir], µM

Figure 3

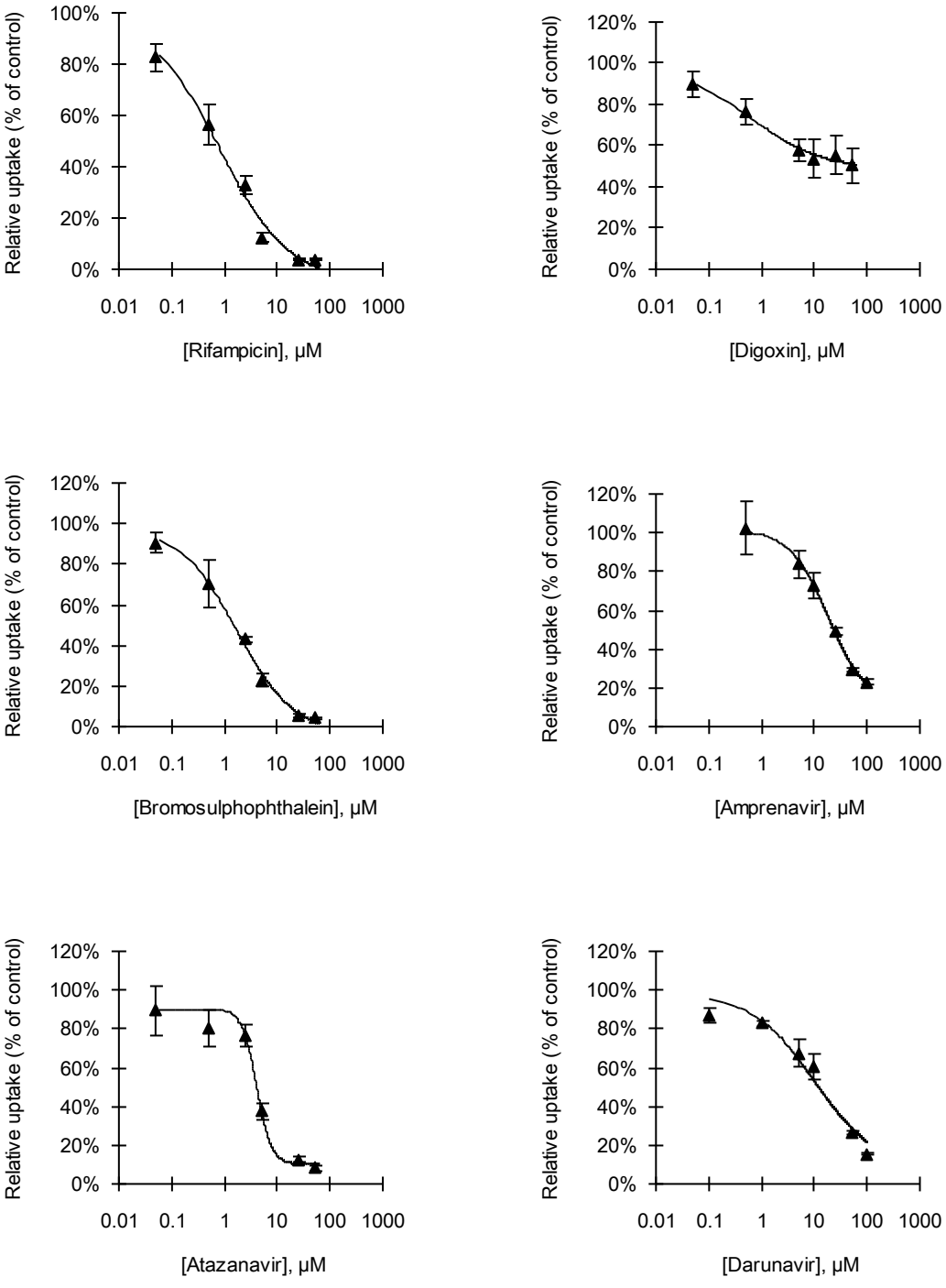

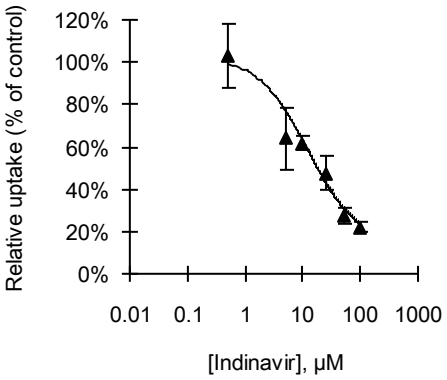
Relative uptake (% of control)
120%
100%
80%
60%
40%
20%
0%
0.01
0.1
1
10
100
1000
[Indinavir], µM

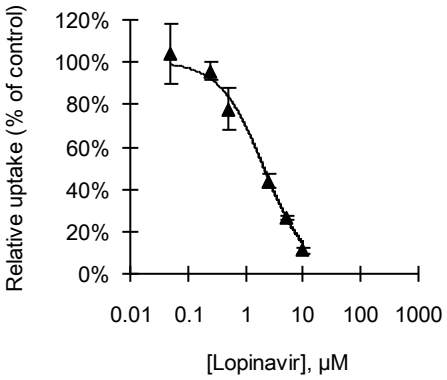
Relative uptake (% of control)
120%
100%
80%
60%
40%
20%
0%
0.01
0.1
1
10
100
1000
[Lopinavir], µM

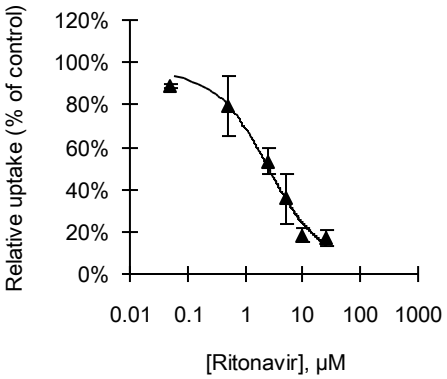
Relative uptake (% of control)
120%
100%
80%
60%
40%
20%
0%
0.01
0.1
1
10
100
1000
[Ritonavir], µM

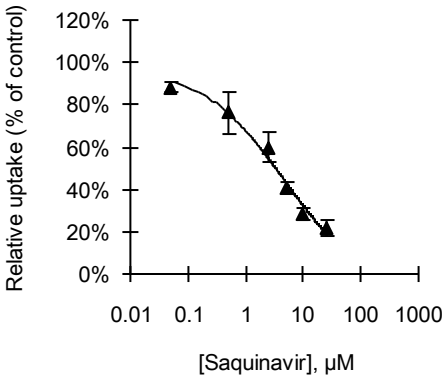
Relative uptake (% of control)
120%
100%
80%
60%
40%
20%
0%
0.01
0.1
1
10
100
1000
[Saquinavir], µM

Figure 4

A

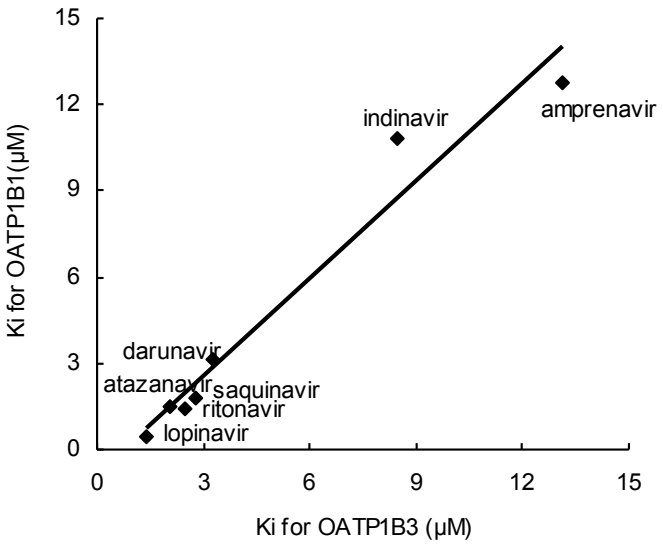

B

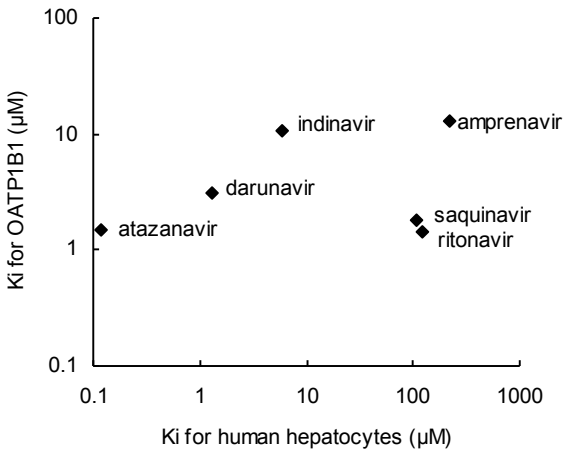

C

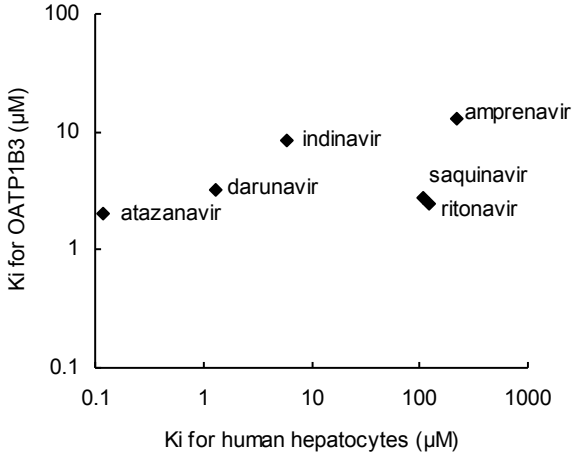

Figure 5

A

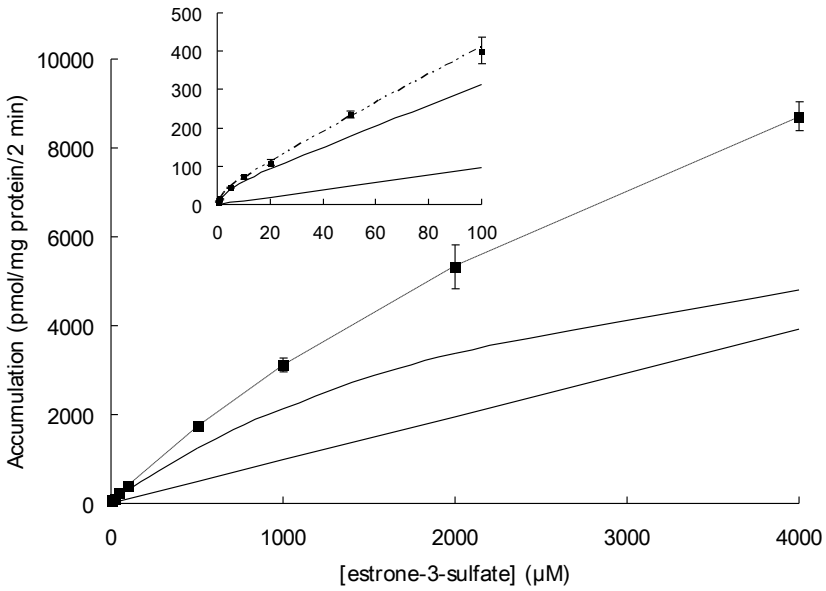

B

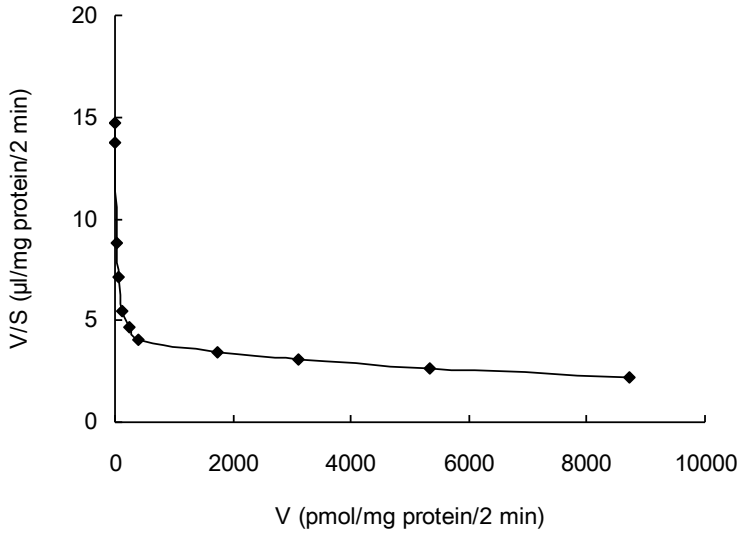

Figure 6

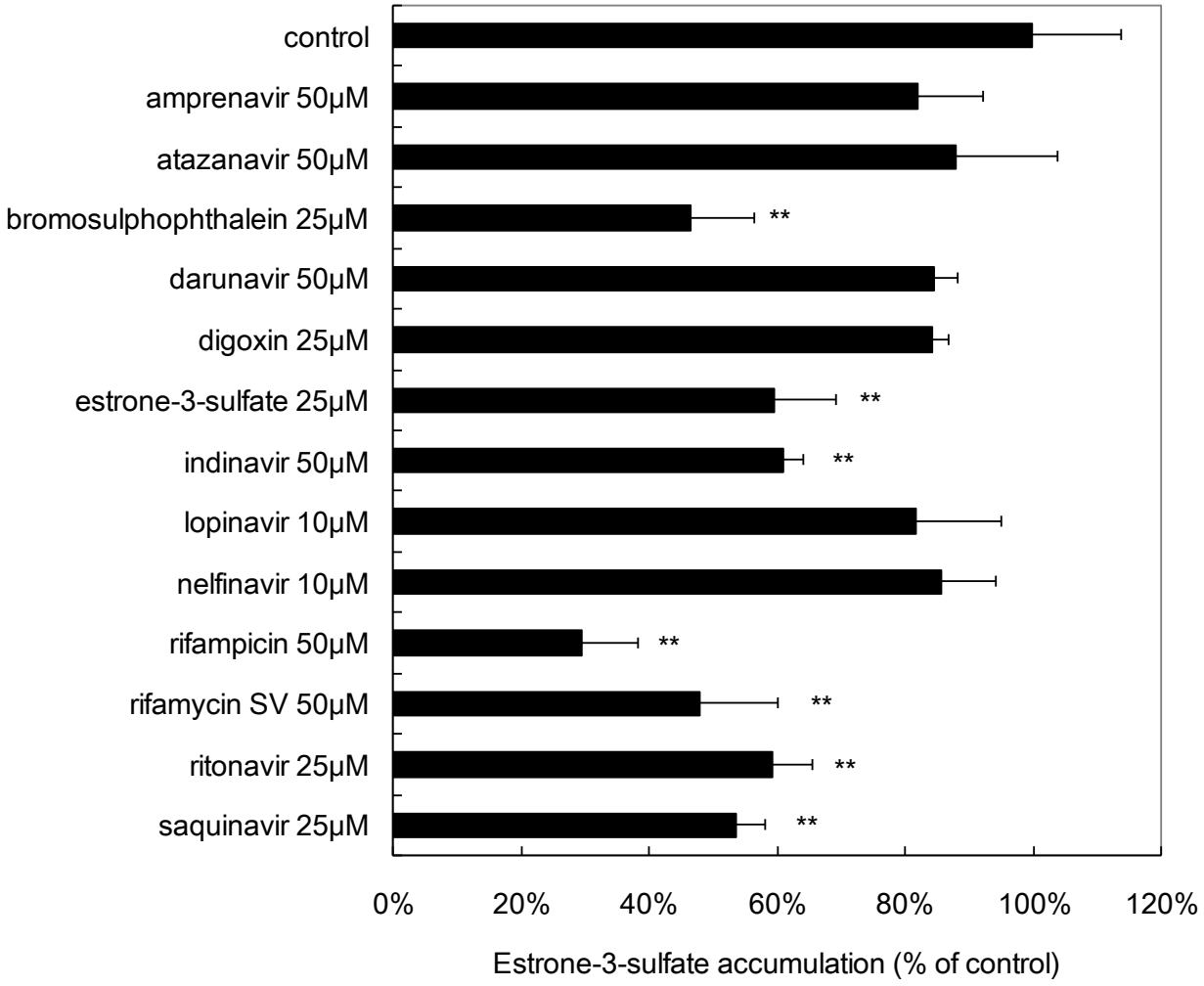
control
amprenavir 50μM
atazanavir 50μM
bromosulphophthalein 25μM
darunavir 50μM
digoxin 25μM
estrone-3-sulfate 25μM
indinavir 50μM
lopinavir 10μM
nelfinavir 10μM
rifampicin 50μM
rifamycin SV 50μM
ritonavir 25μM
saquinavir 25μM
**
0%
20%
40%
60%
80%
100%
120%
Estrone-3-sulfate accumulation (% of control)

Figure 7

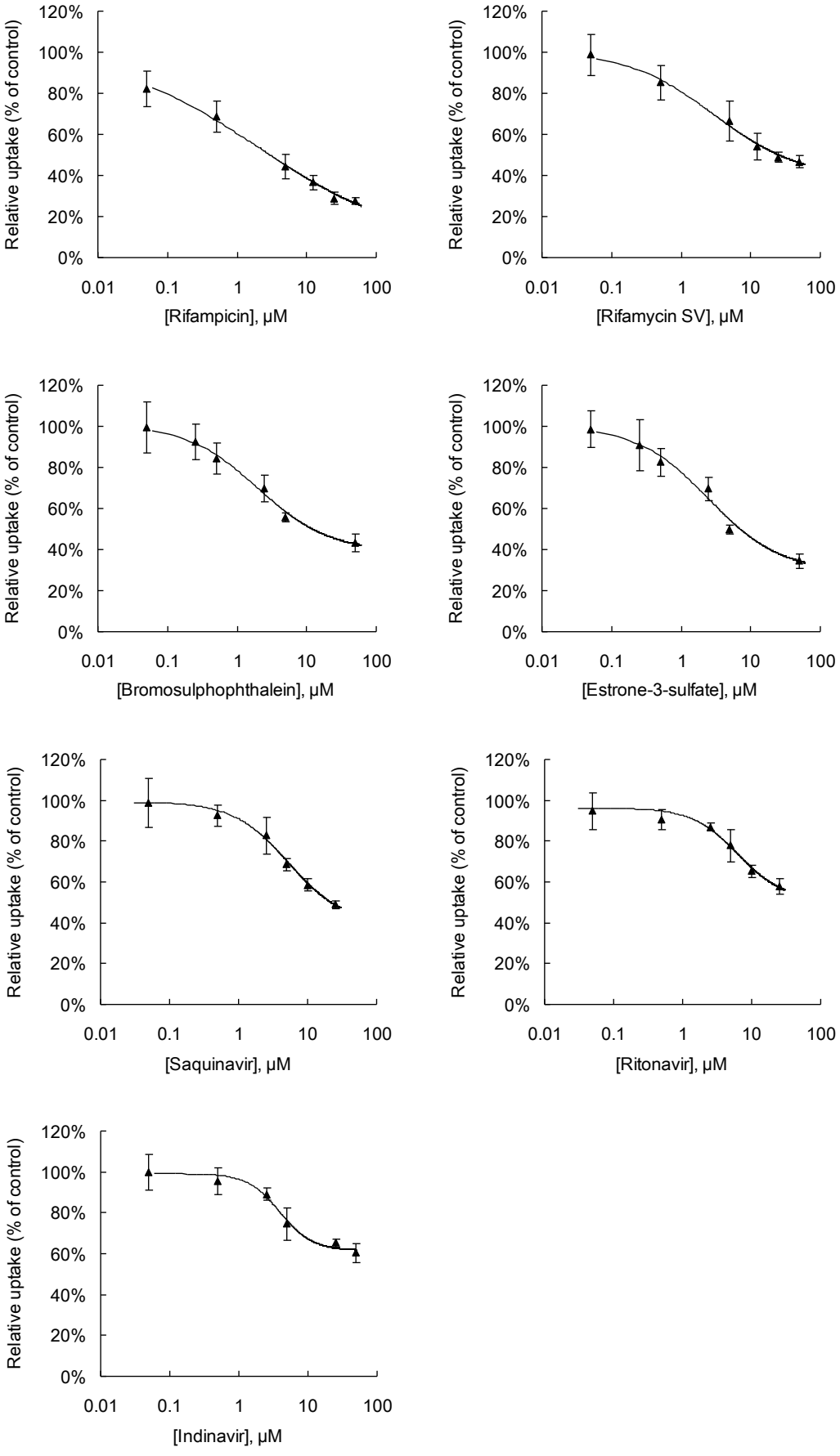
Relative uptake (% of control)
120%
100%
80%
60%
40%
20%
0%
0.01
0.1
1
10
100
[Rifampicin], μM
[Rifamycin SV], μM
[Bromosulphophthalein], μM
[Estrone-3-sulfate], μM
[Saquinavir], μM
[Ritonavir], μM
[Indinavir], μM